

This article was downloaded by:[University of Colorado Libraries]
[University of Colorado Libraries]

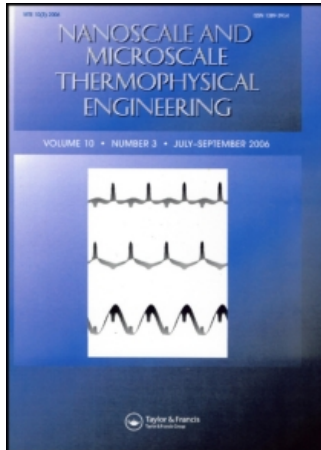
On: 4 June 2007

Access Details: [subscription number 750568220]

Publisher: Taylor & Francis

Informa Ltd Registered in England and Wales Registered Number: 1072954

Registered office: Mortimer House, 37-41 Mortimer Street, London W1T 3JH, UK



Nanoscale and Microscale Thermophysical Engineering

Publication details, including instructions for authors and subscription information:
<http://www.informaworld.com/smpp/title-content=t713774103>

Digitized Heat Transfer Using Electrowetting on Dielectric

To cite this Article: Mohseni, K. and Baird, E.S. , 'Digitized Heat Transfer Using Electrowetting on Dielectric', *Nanoscale and Microscale Thermophysical Engineering*, 11:1, 99 - 108

To link to this article: DOI: 10.1080/15567260701337555

URL: <http://dx.doi.org/10.1080/15567260701337555>

PLEASE SCROLL DOWN FOR ARTICLE

Full terms and conditions of use: <http://www.informaworld.com/terms-and-conditions-of-access.pdf>

This article maybe used for research, teaching and private study purposes. Any substantial or systematic reproduction, re-distribution, re-selling, loan or sub-licensing, systematic supply or distribution in any form to anyone is expressly forbidden.

The publisher does not give any warranty express or implied or make any representation that the contents will be complete or accurate or up to date. The accuracy of any instructions, formulae and drug doses should be independently verified with primary sources. The publisher shall not be liable for any loss, actions, claims, proceedings, demand or costs or damages whatsoever or howsoever caused arising directly or indirectly in connection with or arising out of the use of this material.

© Taylor and Francis 2007

DIGITIZED HEAT TRANSFER USING ELECTROWETTING ON DIELECTRIC

K. Mohseni and E.S. Baird

Aerospace Engineering Sciences, University of Colorado at Boulder, Boulder, Colorado, USA

This paper proposes the use of electrowetting on dielectric (EWOD) as the driving force for digitized heat transfer (DHT), a novel approach to microscale thermal management in which system cooling is actively achieved via the manipulation of an array of discrete microdroplets. Galinstan, a nontoxic, readily available, inexpensive liquid alloy with 65 times less thermal resistance than water, is proposed as a viable DHT coolant. The nature of the EWOD driving force and the velocity of EWOD-actuated droplets are presented, along with an analysis demonstrating the advantages of DHT over some other methods of microscale heat control.

KEY WORDS: digitized heat transfer, microfluidics, electrowetting, thermal management

INTRODUCTION

Heat production is an unavoidable byproduct of the operation of an electronic device. Unfortunately, excess heat can also reduce device performance and durability [1, 2]. As electronic systems become both smaller in size and larger in power consumption, the development of effective methods for small-scale thermal management becomes increasingly vital. Traditionally, heat is removed from an electronic device to the surrounding environment through air-cooled heat sinks. However, liquid coolants, which typically have thermal conductivities much greater than air, can support substantially higher rates of heat flux [3].

Liquids also present a substantial advantage for handling concentrated areas of locally high heat flux known as “hot spots.” We propose a novel method for microscale thermal management in which a programmable array of discrete microdroplets is used to actively manage system cooling; localized hot spots can therefore be specifically and efficiently targeted as they arise. We refer to this technique as “digitized heat transfer” (DHT) [4, 5]. Because DHT does not require a continuous flow, the amount of coolant required and the energy to drive the flow is greatly reduced.

EWOD, in which microdroplets are transported by the application of an electric field normal to the direction of flow, is the most promising method for sustaining DHT currently under research; see Mohseni [6]. EWOD can be used for transporting

The authors would like to acknowledge partial support by AFOSR Contract No. FA9550-05-1-0334 and NSF Contract No. CTS-0540004.

Address correspondence to K. Mohseni, Aerospace Engineering Sciences, University of Colorado at Boulder, 111 Engineering Drive, Room ECAE 197, Boulder, CO 80309-0429. E-mail: mohseni@colorado.edu

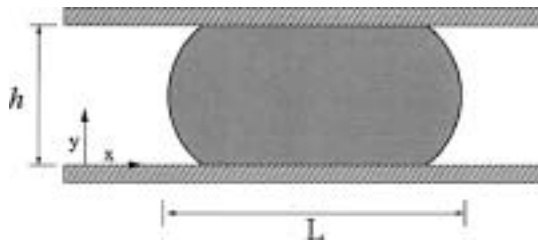


Figure 1. EWOD configuration.

where C is the net capacitance of the dielectric coatings, and V is the applied voltage. The energy in regions of empty channel is negligibly small in the limit of $d \ll h$, which is usually the case for an EWOD device. The EWOD force is generated by lining a channel with electrodes and sequentially firing them such that the leading edge is continually between a charged electrode and ground, whereas the trailing edge is always between grounded electrodes. In this case, the area of the charged capacitor is $A = xw$, where w is the channel width and x is the length of droplet between charged electrodes. The total force on the conductor in any direction can be found by simply differentiating the total energy of the system at fixed potential with respect to the coordinate variable [14–16]:

$$F = \frac{\partial U}{\partial x} \quad (2)$$

Equation (2) is a simple expression of the fact that the work done in moving the conductor a distance dx is equal to the change in energy stored in the electric field. Alternatively, the net force may be calculated by integrating the Maxwell stress tensor around a suitably chosen loop, which will yield the same final result [14–16].

When one side of the channel is lined with a continuous, uninsulated grounding electrode, the droplet is grounded and the total force is directly given by Eqs. (1) and (2),

$$\frac{F}{w} = \frac{1}{w} \frac{\partial U}{\partial x} = \frac{1}{2} c V^2 \quad (3)$$

where c is the capacitance per area of the dielectric layers. Equation (3) is the net forward force, and always serves to draw the droplet into the region of higher electric field.

The scaling of this force is exactly the same as that of surface tension; that is, the net force is directly proportional to the width of the droplet's contact line and is completely independent of the droplet's height or length. For this reason, EWOD dominates actuation methods that scale with the fluid's area or volume, such as pressure or body forces, at sufficiently small length scales.

Note that the EWOD force does not depend on fluid properties such as surface tension or contact angle; the only assumption is that the fluid is considered perfectly conducting. Results for velocity derived below from Eq. (3) will therefore be directly applicable to liquid alloys, in addition to the salt solutions typically used in EWOD experiments. Because of its ability to efficiently transport discrete droplets of thermally and electrically conducting fluids at very small scales, electrowetting on dielectric is an optimum candidate for the driving force of DHT.

DROPLET VELOCITY

In deriving the velocity of EWOD-actuated microdroplets, we consider only the net electrostatic force given by Eq. (3) and substitute this into a simplified momentum equation. To simplify the governing equation, we assume unidirectional, two-dimensional flow such that the only non-zero component of velocity is $u = u(y)$. Numerical simulations in our group suggest this is a valid assumption when $L \gg h$. The droplet is able to translate while simultaneously satisfying a no-slip boundary condition through a dual rolling motion in which the fluid slug is symmetrically split into twin hollow vortices of opposite circulation.

For simplicity, we consider only the EWOD driving force and viscous drag. The one-dimensional Navier-Stokes equation is then given by:

$$\rho \frac{\partial u(y, t)}{\partial t} = \mu \frac{\partial^2 u(y, t)}{\partial y^2} + \frac{1}{2} \frac{cV^2}{hL} \quad (4)$$

The steady-state velocity is found by setting $\frac{\partial}{\partial t} = 0$, integrating twice, and applying the no-slip boundary condition, resulting in:

$$u_{ss}(y) = 6u_{ss}^{avg} \left(\frac{y}{h} - \frac{y^2}{h^2} \right) \quad (5)$$

with

$$u_{ss}^{avg} = \frac{cV^2 h}{24\mu L} \quad (6)$$

as the bulk velocity of the droplet. While the slightly different geometry and the use of silicone oil as an ambient fluid prevent an exact match, both the V^2 dependence and the h/L scaling of Eq. (6) receive concrete experimental verification in Pollack et al. [11].

Contact angle hysteresis may be added to our model if measured values for the advancing and retreating angles are known. With unequal contact angles, a hysteresis force (per unit width), H , is given by the difference in the axial component of surface tension at the front and rear of the droplet:

$$H = \gamma_{lg} [\cos(\theta_a) - \cos(\theta_r)] \quad (7)$$

where a and r stand for advancing and receding, and γ_{lg} is the liquid gas surface tension. When the driving force is below this hysteresis force, no motion is obtained and the droplet remains stationary. This results in a threshold voltage given by

$$V_{thresh}^2 = \frac{8H}{c} \quad (8)$$

and a modified steady-state velocity of

$$u_H^{avg} = \frac{c(V^2 - V_{thresh}^2) h}{24\mu L} \quad (9)$$

above the threshold voltage, where u_H^{avg} represents the average, steady-state droplet velocity with contact angle hysteresis taken into account. The existence of a threshold voltage is also demonstrated in Pollack et al. [11].

Typical EWOD velocities for water droplets range from 10 to 1000 mm/s [8–13]. Galinstan liquid alloy, which has a viscosity roughly twice that of water, is therefore expected to exhibit velocities on the same order of magnitude if the hysteresis effect can be minimized. Preliminary experiments in our group suggest the hysteresis force on a Galinstan droplet is reasonably small when the EWOD device is coated top and bottom with Teflon or another hydrophobic polymer, already a standard practice in EWOD fabrication.

HEAT CONTROL ANALYSIS

A full solution describing digitized heat transfer requires numerically solving the coupled momentum, energy, and continuity equations. To preliminarily identify the basic characteristics of DHT, two drastically simplified treatments are considered. First, the essential heat flux capability of an array of Galinstan droplets is considered from an energy balance perspective. Next, a simplified digital analog to the classic Graetz problem is presented, leading to an extended definition of the Nusselt number for digitized flows. Finally, a numerical treatment of the continuous Graetz problem at low Prandtl number is presented for comparison.

Energy Balance

An energy balance may be applied to determine how the total convective heat transfer Q is related to the difference in temperatures at the channel inlet and outlet. To this end, consider a periodic array of droplets as depicted in Figure 2. Droplets are introduced at a velocity $v = u_H^{avg}$ and with a frequency f at the inlet. If $n = L/\lambda$, one can write $\lambda f = nv$. Since $v = \lambda f$, note that for a fixed droplet velocity, the maximum droplet frequency is $f_{max} = v/L$, corresponding to $n = 1$. For frequencies higher than f_{max} , the flow will be in continuous form and digitized droplets are not feasible. Application of the energy conservation law reveals that

$$Q = mc\Delta T \tag{10}$$

where m is the total mass of droplets, c is the specific heat, and $\Delta T = T_o - T_i$ is the averaged temperature difference between the channel outlet and inlet. Equation (11) can be written in the form of total convective heat transfer rate \dot{Q} as

$$\dot{Q} = \dot{m}c\Delta T \tag{11}$$

or

$$\dot{Q} = \rho f L h w c \Delta T = \rho n v h w c \Delta T \tag{12}$$

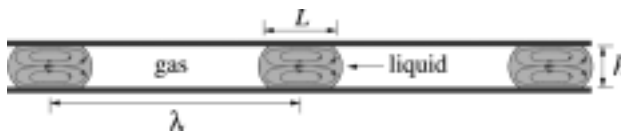


Figure 2. Array of evenly spaced EWOD-activated droplets for DHT. Notice the internal circulation within each droplet which increases heat flux at the walls.

with all variables as defined previously. In this section we are only concerned with the total heat transfer rate and temperature rise of the droplet for a long channel, and consider the two special cases of constant wall temperature T_w and constant wall heat transfer rate \dot{Q}_w .

With T_w constant along a long channel, the droplet temperature at the outlet will approach the wall temperature, $T_o = T_w$. Consequently, the maximum heat transfer rate will be

$$\dot{Q} = \rho f L h w x (T_w - T_i) = \rho n v h w c (T_w - T_i) \quad (13)$$

With \dot{Q}_w held constant, we are interested in estimating the rise in droplet temperature at the outlet. One can easily show that

$$T_o = \frac{\dot{Q}_w}{\rho f L h w c} + T_i = \frac{\dot{Q}_w}{\rho n v h w c} + T_i \quad (14)$$

It is of interest to note the linear dependence of the total heat transfer rate on the droplet velocity v and droplet ratio n .

Conduction Model

In analogy with continuous Graetz flow, we again consider an array of evenly spaced droplets in a channel, as seen in Figure 2. To define the Nusselt number, Nu , as a function of x along the channel, we first consider the temperature of an individual droplet as a function of time.

We assume that each droplet has a uniform temperature profile in the axial direction, and that conduction is the dominant heat transfer mechanism within the droplet. The nondimensionalized heat equation then reduces to Laplace's equation, given by

$$\frac{\partial \theta}{\partial \bar{t}} = \frac{\partial^2 \theta}{d\bar{y}^2} \quad (15)$$

The time coordinate has been nondimensionalized by h^2/k , where k is the heat conduction coefficient of the fluid, the y coordinate has been nondimensionalized by h , and

$$\theta = \frac{T - T_w}{T_i - T_w} \quad (16)$$

T_i and T_w are as given previously. We again apply the isothermal Dirichlet boundary condition of $T_w = \text{Cons}$. An exact solution to Eq. (15) under the above boundary and initial condition is readily given by the Fourier series:

$$\theta = \sum_n c_n \sin(n\pi\bar{y}) e^{n^2\pi^2\bar{t}} \quad (17)$$

with

$$c_n = \frac{-2[1 - (-1)^n]}{n\pi} \quad (18)$$

The average temperature of the droplet, given by integrating over the \bar{y} coordinate, is

$$\theta_{avg}(t) = \sum_n A_n e^{n^2 \pi^2 \bar{t}} \tag{19}$$

with the coefficients A_n given by

$$A_n = \frac{-4[1 - (-1)^n]}{n^2 \pi^2} \tag{20}$$

Finally, the temperature gradient, evaluated at either wall, is given by:

$$\frac{\partial \theta}{\partial y} = \sum_n c_n n \pi e^{n^2 \pi^2 \bar{t}} \tag{21}$$

The Nusselt number of any individual droplet, given as a function of time measured from the moment it enters the heated region, is simply the ratio of the temperature gradient, evaluated at the wall, to the difference in the droplet's average bulk temperature and the wall temperature. A plot of this result is given in Figure 3. The asymptotic value is calculated to be $Nu = 4.935$. This is to be compared with numerically obtained plots of the Nusselt number for continuous Graetz flow, given in Figure 4.

This Nusselt number can be expressed as a function of x along the channel as well. A patch of channel a distance x from the entrance will be passed over by droplets which have been in the channel an average time of $t = x/u_{ss}^{avg}$, where t is the full, dimensional time. The patch will be covered by a droplet, on average, a fraction L/λ of the time. By substituting in basic definitions, it is seen that

$$\frac{x/h}{\text{Re Pr}} = \frac{u_{ss}^{avg} t}{h} \frac{\nu}{u_{ss}^{avg} h} \frac{\kappa}{\nu} = \frac{kt}{h^2} = \bar{t} \tag{22}$$

Therefore, $\frac{x/h}{\text{Re Pr}}$, the usual nondimensionalized spatial variable used in plotting the Nusselt number, is equivalent to the dimensionless temporal variable associated with a droplet moving down the channel. This approximate result extends the concept of

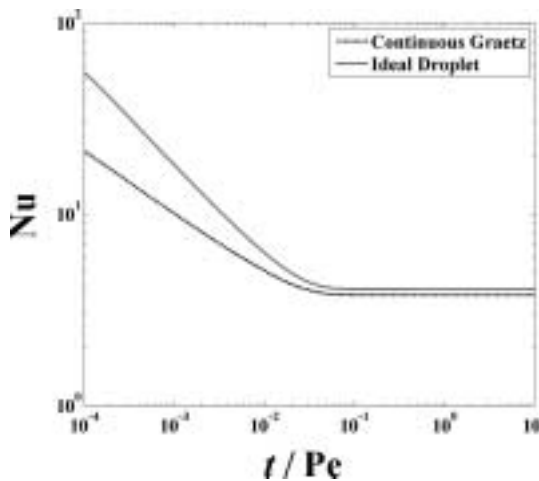


Figure 3. Conduction model Nusselt number for an idealized droplet array (solid), with Nusselt number for classical Graetz flow (dashed).

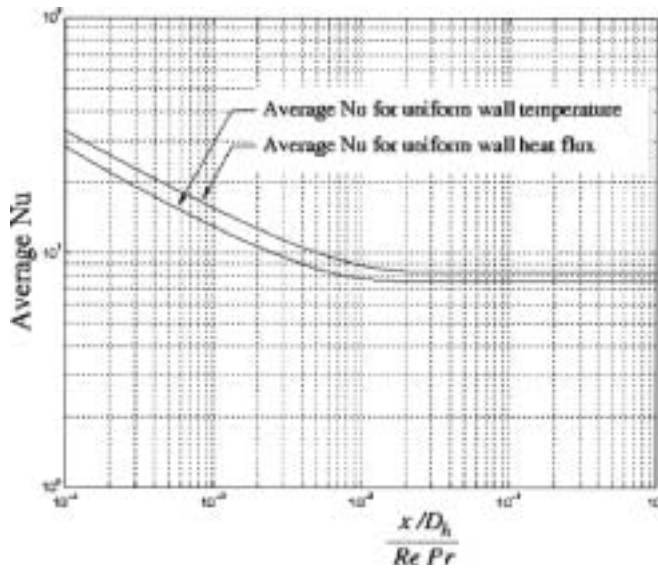


Figure 4. Numerically obtained Nusselt number for continuous Graetz flow.

Nusselt number to an array of discrete droplets. For a real droplet, internal mixing will convect heat away from the walls toward the droplet's center, leading to a more uniform temperature profile. It is therefore expected that real droplets will have a higher average heat flux at the walls, and the Nusselt number will be somewhat greater than in Figure 3.

While the models presented in this section are crude, they nevertheless provide meaningful insight into the properties of a discretized flow. Results for Nusselt number, for instance, closely follow the trend of the exact solution to the continuous Graetz problem. More detailed numerical simulations are expected to produce results of the same order of magnitude with the same basic scaling properties, providing a preliminary check on the physical validity of a numerical result.

Continuous Graetz Flow

In most cases, electrostatically actuated flows in microchannels are expected to be laminar. Correlations for the average Nusselt number in continuous flow in microchannels in terms of Prandtl and Reynolds numbers have been reported in the literature [17–19]. In general, significant variations have been observed in these correlations. Many possible explanations for such deviations from classical theory have been suggested. These include relative surface roughness of the microchannels and the entrance effect. While for high Prandtl number fluids extensive theoretical and experimental data are available, low Prandtl number data are scarce. Accurate numerical simulation of low Prandtl number flow with applications to digitized heat transfer is a topic of future investigation.

In this section, a simplified comparison of laminar heat transfer in micro pipes is offered in order to highlight significant heat transfer enhancement by the use of liquid alloys or metals instead of water. We consider steady laminar flow in two dimensions

between parallel plates. One of the walls represents the hot surface of an electronic device. We assume that the flow is fully developed hydrodynamically, but not thermodynamically. The range of variations in the coolant temperature is small enough that constant fluid properties can be assumed. Such a flow is the plane version of thermally developing flow, often known as the Graetz problem [20].

We consider the two cases of constant wall temperature T_w and constant wall flux q_w . The coolant enters the heated region at a uniform temperature of T_i . The droplet velocity is assumed to follow a parabolic profile, and the nondimensionalized energy equation can then be reduced to

$$\frac{\partial \theta}{\partial \bar{x}} = \frac{1}{U} \frac{\partial^2 \theta}{\partial \bar{y}^2} \quad (23)$$

with

$$\bar{x} = \frac{x/h}{\text{Re Pr}} \quad (24)$$

and θ and \bar{y} as defined previously. Note that $\text{Re} = Uh / \nu$. Since the velocity field is assumed fully developed, no radial velocity component appears in this equation. This equation can be solved numerically using the appropriate boundary and entrance conditions. A finite difference method is employed to solve these equations. The results are shown in Figure 4.

CONCLUSIONS

This article has proposed the use of electrowetting on dielectric as the driving force for a new method of micro scale thermal management dubbed as digitized heat transfer. The nature of the EWOD force and the velocity of EWOD-actuated droplets were derived. Conducting liquids, especially Galinstan liquid alloy, are seen to represent a significant improvement in cooling power over air due to their orders of magnitude higher values of thermal mass and thermal conductivity. EWOD is shown to be a viable option for transporting droplets of such fluids, and a simple analysis characterizes the Nusselt number for a discrete microdroplet array. The simple equations for EWOD velocities presented in this document are directly applicable to a wide spectrum of microfluidic technologies, and the efficient, active management technique of DHT is a promising technique for future research.

REFERENCES

1. A. Bar-Cohen, A. Kraus, and S. Davidson Thermal Frontiers in the Design and Packaging of Microelectronic Equipment, *Mechanical Engineering*, vol. 6, pp. 53–59, 1983.
2. Reliability Prediction of Electronic Equipment, DOD paper MIL-HDBK-217C, New York, 1980.
3. D. Tuckerman and R. Pease, High Performance Heat Sinking for VLSI, *IEEE Electron Device Letters*, vol. 2, pp. 126–129, 1981.
4. A. Dolatabadi, K. Mohseni, and A. Arzpeyma, Behavior of a Moving Droplet under Electrowetting Actuation: Numerical Simulation, *Canadian Journal of Chemical Engineering*, vol. 84, pp. 17–21, 2006.

5. K. Mohseni, E. Baird, and H. Zhao, Digitized Heat Transfer for Thermal Management of Compact Microsystems, IMECE 2005-79372, Orlando, FL, November 2005.
6. K. Mohseni, Effective Cooling of Integrated Circuits Using Liquid Alloy Electrowetting, *Proc. 21st SemiTherm Symp.*, pp. 20–25, 2005.
7. V. Pamula and K. Chakrabarty, Cooling of Integrated Circuits Using Droplet-Based Microfluidics, *Proc. ACM Great Lakes Symposium on VLSI*, pp. 84–87, 2003.
8. S. Cho, H. Moon, and C. Kim, Creating, Transporting, Cutting, and Merging Liquid Droplets by Electrowetting-Based Actuation for Digital Microfluidic Circuits, *Journal of Microelectromechanical Systems*, vol. 12, pp. 70–80, 2003.
9. C. Cooney, C.-Y. Chen, M. Emerling, A. Nadim, and J. Sterling, Electrowetting Droplet Microfluidics on a Single Planar Surface, *Journal of Microfluidics and Nanofluidics*, Vol. 2, pp. 435–446, 2006.
10. T. Jones, An Electromechanical Interpretation of Electrowetting, *Journal of Micromechanics and Microengineering*, vol. 15, pp. 1184–1187, 2006.
11. M. Pollack, A. Shenderov, and R. Fair, Electrowetting-Based Actuation of Droplets for Integrated Microfluidics, *Lab on a Chip*, vol. 2, pp. 96–101, 2002.
12. B. Shapiro, H. Moon, R. Garrel, and C. Kim, Equilibrium Behavior of Sessile Drops under Surface Tension, Applied External Fields, and Material Variations, *Journal of Applied Physics*, vol. 93, pp. 5794–5811, 2003.
13. K. Wang and T. Jones, Electrowetting Dynamics of Microfluidic Actuation, *Langmuir*, vol. 21, pp. 4211–4217, 2005.
14. D. Griffiths, *Introduction to Electrodynamics*, Prentice Hall, Englewood Cliffs, NJ, 1999.
15. L. Landau and E. Lifshitz, *Electrodynamics of Continuous Media*, Pergamon Press, Oxford NY, 1960.
16. J. Jackson, *Classical Electrodynamics*, 3rd Ed., John Wiley and Sons, Inc., New York, 1999.
17. G. Duncan and G. Peterson, Review of Microscale Heat Transfer, *Applied Mechanics Reviews*, vol. 47(9), pp. 397–428, 1994.
18. N. Obot, Toward a Better Understanding of Friction and Heat/Mass Transfer in Microchannels—A Literature Review, *Microscale Thermophysical Engineering*, vol. 6, pp. 155–173, 2002.
19. C. Sobhan and S. Garimella, A Comparative Analysis of Studies on Heat Transfer and Fluid Flow in Microchannels, *Microscale Thermophysical Engineering*, vol. 5, pp. 293–311, 2001.
20. A. Bejan, *Convection Heat Transfer*, 2nd Ed., Wiley-Interscience, New York, 1994.